

# Bayesian Estimation of Equivalent Circuit Parameters of Photovoltaic Cell with S-Shaped Current–Voltage Characteristic

Kazuya Tada

An S-shaped current–voltage characteristic is frequently observed in a photovoltaic cell using emerging materials such as organic semiconductors and organic–inorganic perovskite materials. The opposed two-diode equivalent circuit model, whose explicit analytical solution is known, can reproduce the S-shaped characteristic. However, since the number of parameters is as high as eight, it is not easy to extract the equivalent circuit parameters from experimental data by curve fitting. Herein, the Bayesian estimation in extracting the equivalent circuit parameters of the opposed two-diode model is demonstrated. Unlike the traditional nonlinear least-squares method, the Bayesian estimation practically does not require any tuning of the initial values and gives the information on the error of the estimates.

## 1. Introduction

The photovoltaic cell is an essential technology for the sustainable development of society. The equivalent circuit model of a photovoltaic cell is a useful tool for clarifying the mechanism of losses inside a photovoltaic cell. Moreover, the model is beneficial for the design of devices using photovoltaic cells because it can represent the current–voltage characteristics of photovoltaic cells with a limited number of parameters. For this reason, technology for extracting the equivalent circuit parameters of photovoltaic cells from the experimentally obtained current–voltage characteristics of photovoltaic cells has been extensively studied.<sup>[1–3]</sup>

In a photovoltaic cell using emerging materials such as organic semiconductors and organic–inorganic perovskite materials, an S-shaped current–voltage characteristic is frequently observed. To understand this phenomenon, the opposed two-diode model shown in **Figure 1** has been proposed.<sup>[4–6]</sup> In this model, a diode  $D_2$  is connected in series with the one-diode model, which is in the opposite direction to the diode  $D_1$  in the basic one-diode model, and  $D_2$  is accompanied by a parallel resistor  $R_{p2}$ . The second diode  $D_2$  is intended to model an imperfect metal/semiconductor interface and is often assigned

significantly larger ideality factor than  $D_1$ . It has also been recommended that the series resistance  $R_s$  be neglected to make fitting easier by reducing the number of parameters. However, in a previous article, the author showed that the ideality factor  $n_2$  for  $D_2$  does not have to be large and that ignoring  $R_s$  significantly increases the fitting error.<sup>[7]</sup>

The nonlinear least-squares method is routinely used to extract the equivalent circuit parameters.<sup>[8–10]</sup> However, this method is characterized by the fact that it can only provide point estimates that depend on the initial values. Therefore,

it is necessary to tune the initial value to obtain an appropriate estimate. Furthermore, since it is a point estimate, it is not clear how much error should be assumed in the estimated value. These are the well-known general problems in the curve-fitting of experimental data. As a solution to these problems, parameter extraction using Bayesian estimation has been proposed and has produced remarkable results in various fields of science and technology.<sup>[11–13]</sup> Recently, the author reported that the Bayesian estimation is also effective in extracting the equivalent circuit parameters of the one-diode model of a photovoltaic cell.<sup>[14]</sup>

In this article, we used the Bayesian estimation to extract the equivalent circuit parameters in the opposed two-diode model of a photovoltaic cell. In the Bayesian estimation, it is necessary to search the space of the dimension of the number of parameters. Therefore, the two-diode model with eight parameters is a challenging task, since it is more difficult to estimate the parameters than the one-diode model with five parameters.

In the previous article,<sup>[7]</sup> it has been shown that whether the ideality factor of  $D_2$  ( $n_2$ ) is the same as that of  $D_1$  ( $n_1$ ) (case1:  $n_1 = n_2 = 1.92$ ) or very larger than  $n_1$  (case2:  $n_1 = 1.00$ ,  $n_1 = 3.00$ ), the nonlinear least-squares method finds a set of equivalent circuit parameters that reproduces the experimental data of an organic photovoltaic cell, as shown in **Figure 2**. Note that the currents and equivalent circuit parameters in this article are normalized to the unit area ( $1 \text{ cm}^2$ ).

This result means that it is not possible to determine what value of the diode ideality factors are reasonable as long as the nonlinear least-squares method is used. In other words, unless we put in very small values for  $n_1$  and  $n_2$ , the nonlinear least-squares method gives a set of equivalent circuit parameters with a small enough error. This implies that some parameters, such as the diode ideality factors, cannot be determined definitively because the model has eight parameters and is very flexible.

K. Tada

Department of Electrical Materials and Engineering  
University of Hyogo  
2167 Shosha, Himeji, Hyogo 671-2280, Japanhyogo  
E-mail: tada@eng.u-hyogo.ac.jp

 The ORCID identification number(s) for the author(s) of this article can be found under <https://doi.org/10.1002/pssa.202100403>.

DOI: 10.1002/pssa.202100403

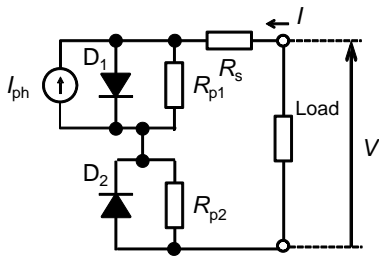


**Figure 1.** Opposed two-diode equivalent-circuit model of a photovoltaic cell.

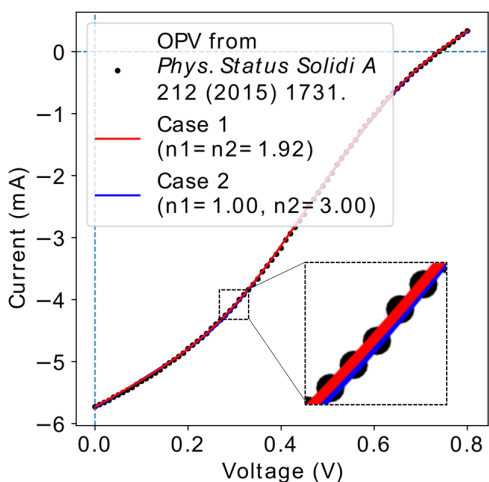


**Figure 2.** Fitting results for the experimental current density–voltage characteristic (symbols) of an organic photovoltaic cell from ref. [7]. In case 1 (blue solid line) and case 2 (red dashed line),  $n_1 = n_2 = 1.92$  and  $n_1 = 1.00$  as well as  $n_2 = 3.00$  were respectively assumed.

Based on this finding, we will focus on the following two points in the present study. First, we check whether the Bayesian estimation can discriminate between the two theoretical curves obtained from the aforementioned cases 1 and 2, which are apparently indistinguishable. Second, we investigate whether the Bayesian estimation from the measured data can estimate the ideality factor of each diode within a sufficiently narrow range.

## 2. Models and Methods

Practical Bayesian estimation involves the computation of multidimensional integrals of complicated functions, and thus requires sampling such as Markov Chain Monte Carlo (MCMC) methods. One of the most efficient MCMC algorithms at present is NUTS (No-U-Turn Sampler),<sup>[15]</sup> which is implemented in PyMC3, the software package used in this article, as a standard method.<sup>[16]</sup> The analytical solution  $V(I)$  of the opposed two-diode equivalent circuit model shown in Figure 1 is obtained using Lambert W-function, defined as the solution of  $W(z) \cdot \exp(W(z)) = z$ .<sup>[17,18]</sup> However, this expression has the disadvantage that it tends to deviate from the range of numbers that can be represented by standard 64-bit floating-point

format because it contains exponential functions for large numbers. To avoid this, the g-function  $g(x) = \ln(W(\exp(x)))$  proposed by Roberts is used in this article.<sup>[19]</sup> The analytical solution  $V(I)$  using the g-function is as follows<sup>[20]</sup>

$$V(I) = I \cdot R_s + n_1 \cdot V_t \cdot \left( g(x_1(I)) - \ln\left(\frac{I_{01} \cdot R_{p1}}{n_1 \cdot V_t}\right) \right) - n_2 \cdot V_t \cdot \left( g(x_2(I)) - \ln\left(\frac{I_{02} \cdot R_{p2}}{n_2 \cdot V_t}\right) \right) \quad (1)$$

with

$$x_1(I) = \ln\left(\frac{I_{01} \cdot R_{p1}}{n_1 \cdot V_t}\right) + \frac{(I + I_{01} + I_{ph}) \cdot R_{p1}}{n_1 \cdot V_t} \quad (2)$$

and

$$x_2(I) = \ln\left(\frac{I_{02} \cdot R_{p2}}{n_2 \cdot V_t}\right) - \frac{(I - I_{02}) \cdot R_{p2}}{n_2 \cdot V_t} \quad (3)$$

The subscripts 1 and 2 for the ideality factor  $n$  and the reverse saturation current  $I_0$  correspond to  $D_1$  and  $D_2$ , respectively. The thermal voltage  $V_t$  is  $\approx 26$  mV at room temperature. Other parameters are mentioned in Figure 1. The implementation of the g-function in PyMC3 is described in ref. [14] in detail.

Unless otherwise noted, in all of the following cases, the prior probability distribution for each parameter was set to be a uniform probability in the range of several orders of magnitude as shown here. The reason for the strict upper and lower bounds is to eliminate the possibility of overflow in the calculation of  $V(I)$ .

$$I_{ph}[\text{mA}] \sim \text{Unif}(1 \times 10^{-3}, 1 \times 10^2) \quad (4)$$

$$R_s[\Omega] \sim \text{Unif}(1 \times 10^{-1}, 1 \times 10^3) \quad (5)$$

$$R_{p1}[\Omega] \sim \text{Unif}(1 \times 10^1, 1 \times 10^4) \quad (6)$$

$$I_{01}[\text{pA}] \sim \text{Unif}(1 \times 10^{-4}, 1 \times 10^7) \quad (7)$$

$$n_1 \sim \text{Unif}(5 \times 10^{-1}, 1 \times 10^2) \quad (8)$$

$$R_{p2}[\Omega] \sim \text{Unif}(1 \times 10^1, 1 \times 10^4) \quad (9)$$

$$I_{02}[\text{pA}] \sim \text{Unif}(1 \times 10^2, 1 \times 10^{10}) \quad (10)$$

$$n_2 \sim \text{Unif}(5 \times 10^{-1}, 1 \times 10^2) \quad (11)$$

To promote convergence, sampling was performed with the MAP (maximum a posteriori) estimate, which gives a point estimate of the set of parameters, as the initial value. The MCMC method requires discarding samples before reaching a stationary distribution, which is called burn-in. Obtaining essentially identical posterior probability distributions from multiple parallel computations (chains) supports the validity of the result. In all cases, after 10 000 burn-in periods, 10 000 samples were taken over four chains. Each calculation took approximately half a day on a computer equipped with an Intel Core i9 CPU running at about 3.0 GHz. This is approximate twice the time required to estimate the one-diode model reported in ref. [14], where the number of samples was an order of magnitude larger.

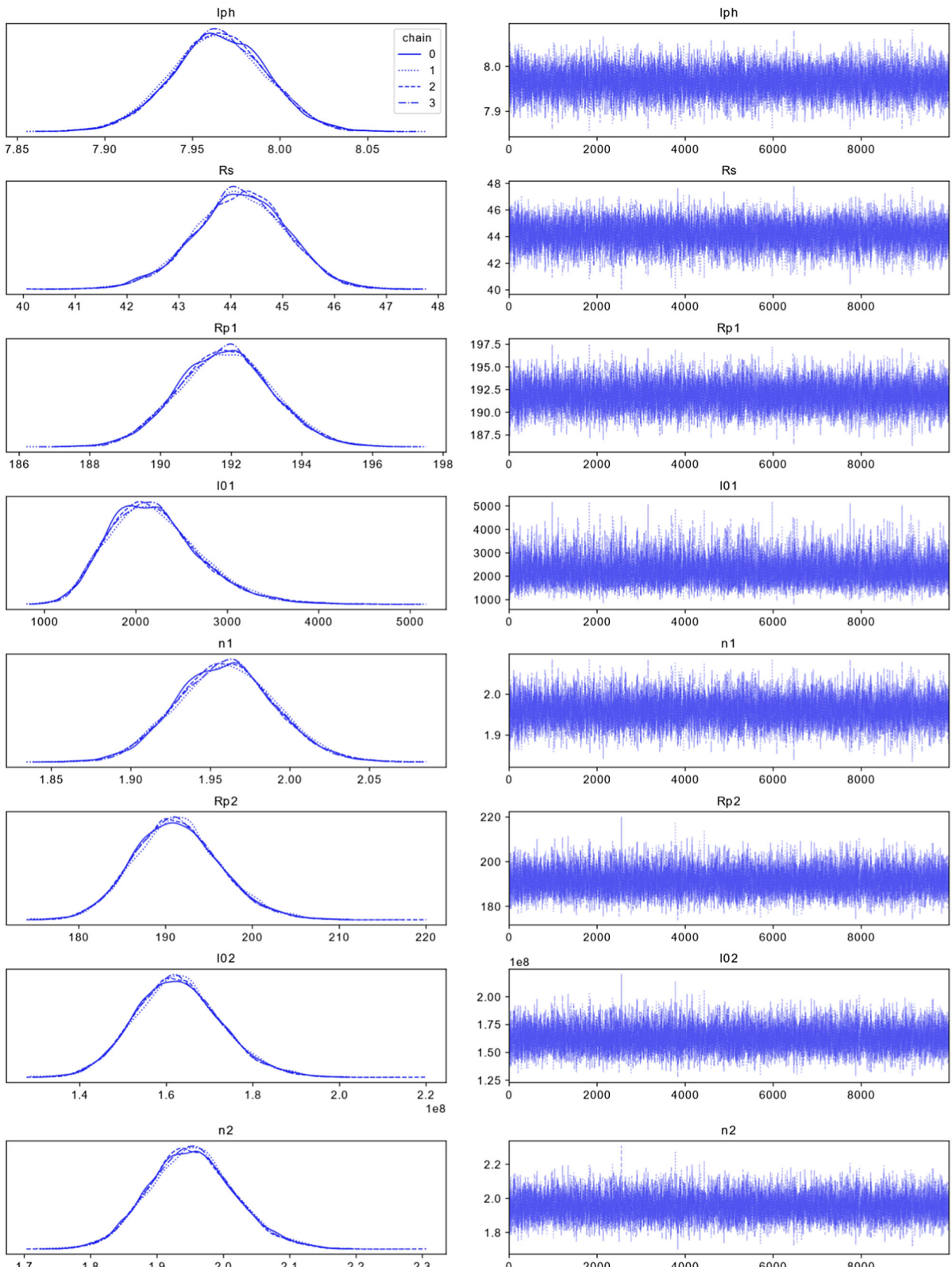


**Figure 3.** Kernel density estimates (left panels) and simulated traces (right panels) for each equivalent circuit parameter of the theoretical curve generated using the parameters of case 1.

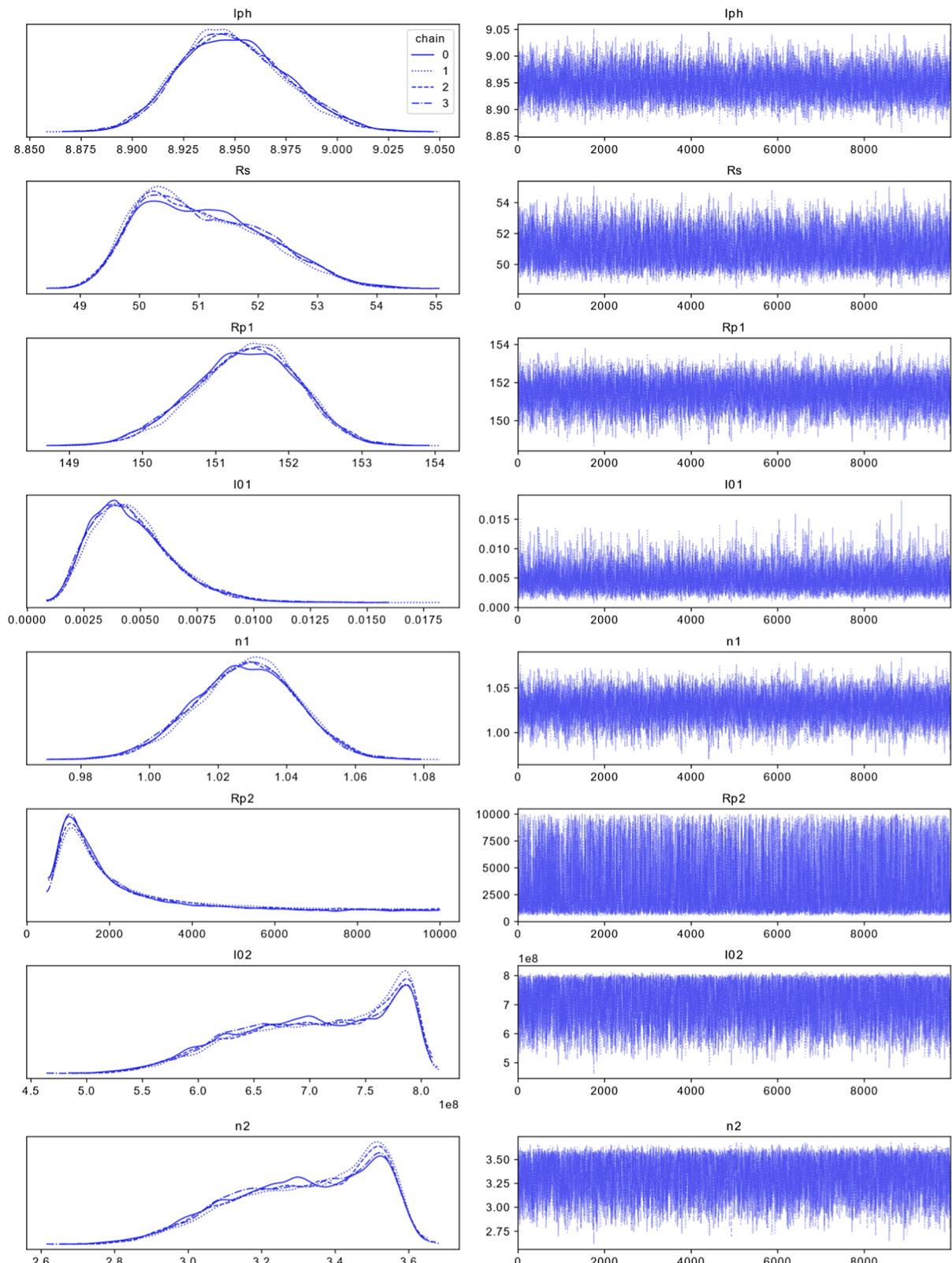


**Figure 4.** Kernel density estimates (left panels) and simulated traces (right panels) for each equivalent circuit parameter of the theoretical curve generated using the parameters of case 2.

### 3. Results and Discussion

#### 3.1. Discriminating the Difference Between Two Almost Identical Theoretical Curves

**Figure 3** shows the results of Bayesian estimation for the theoretical curve generated using the case 1 parameters. For this calculation, we used the data with Gaussian noise of  $1 \times 10^{-6}$  A for the current to simulate the experimental error. It has been observed that if the noise is increased too much, the calculation does not converge properly. Each panel on the left side shows the kernel density estimate corresponding to the probability density distribution of each parameter, which reproduces the given data. According to the central limit theorem, if the number of sampling is sufficiently large, the shape of a kernel density estimate approaches a normal distribution. In each panel on the right side, trace plot for each parameter is shown. The fact that the trace is busily moving around a certain range is a strong piece of evidence that the calculation is converging well. The vertices of the kernel density estimates of the estimates of  $n_1$  and  $n_2$  in Figure 3 are around 2, indicating that the values used for the generation of theoretical curve are estimated correctly.

**Figure 4** shows the results of Bayesian estimation for the theoretical curve generated using the parameters of case 2. For this calculation, we also added Gaussian noise of  $1 \times 10^{-6}$  A for the theoretical value of the current, just as we did for case 1. The kernel density estimates shown in the left panels and the trace plots shown in the right panels have the same features as those shown in Figure 3, indicating that they are well sampled. Interestingly, the vertices of the kernel density estimates estimated for  $n_1$  and  $n_2$  in Figure 4 are found around 1 and 3, respectively, indicating that they correctly estimate the given theoretical values.

**Table 1** summarizes the theoretical values of each parameter, as well as the mean and standard deviation obtained by the Bayesian estimation. Although the mean values deviate slightly from the theoretical values due to the given noise, they are generally equal to the theoretical values. Thus, we can conclude that the Bayesian estimation can correctly distinguish the difference between the two theoretical curves shown in Figure 2, which look almost identical. In other words, the Bayesian estimation on the two curves generated from the parameters extracted by the

least-squares method is able to make good estimates of the parameters used to generate the curve.  $\hat{R}$  is a key indicator of convergence of the calculation, and it is close to 1.0 when it is appropriately converged.

#### 3.2. Extraction of Equivalent Circuit Parameters from Measured Data

**Figure 5** shows the results of Bayesian estimation for the measured data presented in ref. [21]. To obtain this result, we set  $R_s = 0$  and also increased the upper bound of the prior probability distribution for  $I_{01}$  by one order of magnitude. The reason for this is as follows. When the same prior probability distribution was used as before, the kernel density estimates for  $I_{01}$  became a monotonically increasing curve with no vertices. However, simply increasing the upper limit of the prior probability distribution for  $I_{01}$  by an order of magnitude resulted in a monotonically decreasing curve with no vertices for the kernel density estimate for  $R_s$ . Since  $R_s$  is not negative, this result can be interpreted as the average value of estimated  $R_s$  being less than  $0.1 \Omega$  and practically zero. Under this condition, the kernel density estimate of each parameter has a shape close to the normal distribution, as shown in Figure 5. It is worth noting that the result  $R_s = 0$  in this article, was derived by chance, and it is not recommended to ignore  $R_s$  beforehand when modeling the S-shaped current-voltage characteristics in the opposing two-pole model. For example, the change of  $R_s$  plays a key role in previous studies.<sup>[22]</sup>

**Table 2** summarizes the means and standard deviations obtained by Bayesian estimation for each parameter. The ideality factors of the diodes  $n_1$  and  $n_2$  are estimated within a sufficiently narrow range, that is, we have successfully determined the ideality factor of each diode from the measured data, which was difficult to do with the least-squares method. It can be confirmed that the fitting curve using the mean values reproduces the measured data well, as shown in **Figure 6**.

In previous studies, it has been assumed that  $n_1$  is smaller than  $n_2$ . This is because it has been believed that  $D_1$  represents a healthy metal/semiconductor interface and  $D_2$  models some imperfection of the interface. However, the Bayesian estimation predicts that  $n_1$  is larger than  $n_2$ , suggesting that  $D_2$  is healthier than  $D_1$ . Although this is an interesting result, the physical

**Table 1.** True values and Bayesian estimation of the equivalent circuit parameters of cases 1 and 2.

True value	Case 1			Case 2		
	Bayesian estimation		$\hat{R}$	True value	Bayesian estimation	
	Mean value	Standard deviation			Mean value	Standard deviation
$I_{ph}$ [mA]	8.00	7.97	0.03	1.0	9.00	8.95
$R_s$ [ $\Omega$ ]	45.0	44.2	0.9	1.0	53.0	51.1
$R_{p1}$ [ $\Omega$ ]	$1.90 \times 10^2$	$1.92 \times 10^2$	$0.01 \times 10^2$	1.0	$1.50 \times 10^2$	$1.51 \times 10^2$
$I_{01}$ [pA]	$1.60 \times 10^3$	$2.20 \times 10^3$	$0.51 \times 10^3$	1.0	$2.00 \times 10^{-3}$	$5.00 \times 10^{-3}$
$n_1$	1.92	1.96	0.03	1.0	1.00	1.03
$R_{p2}$ [ $\Omega$ ]	$1.90 \times 10^2$	$1.91 \times 10^2$	$0.05 \times 10^2$	1.0	$8.40 \times 10^2$	$2.96 \times 10^3$
$I_{02}$ [pA]	$1.60 \times 10^8$	$1.63 \times 10^8$	$0.10 \times 10^8$	1.0	$6.00 \times 10^8$	$7.07 \times 10^8$
$n_2$	1.92	1.95	0.07	1.0	3.00	3.32

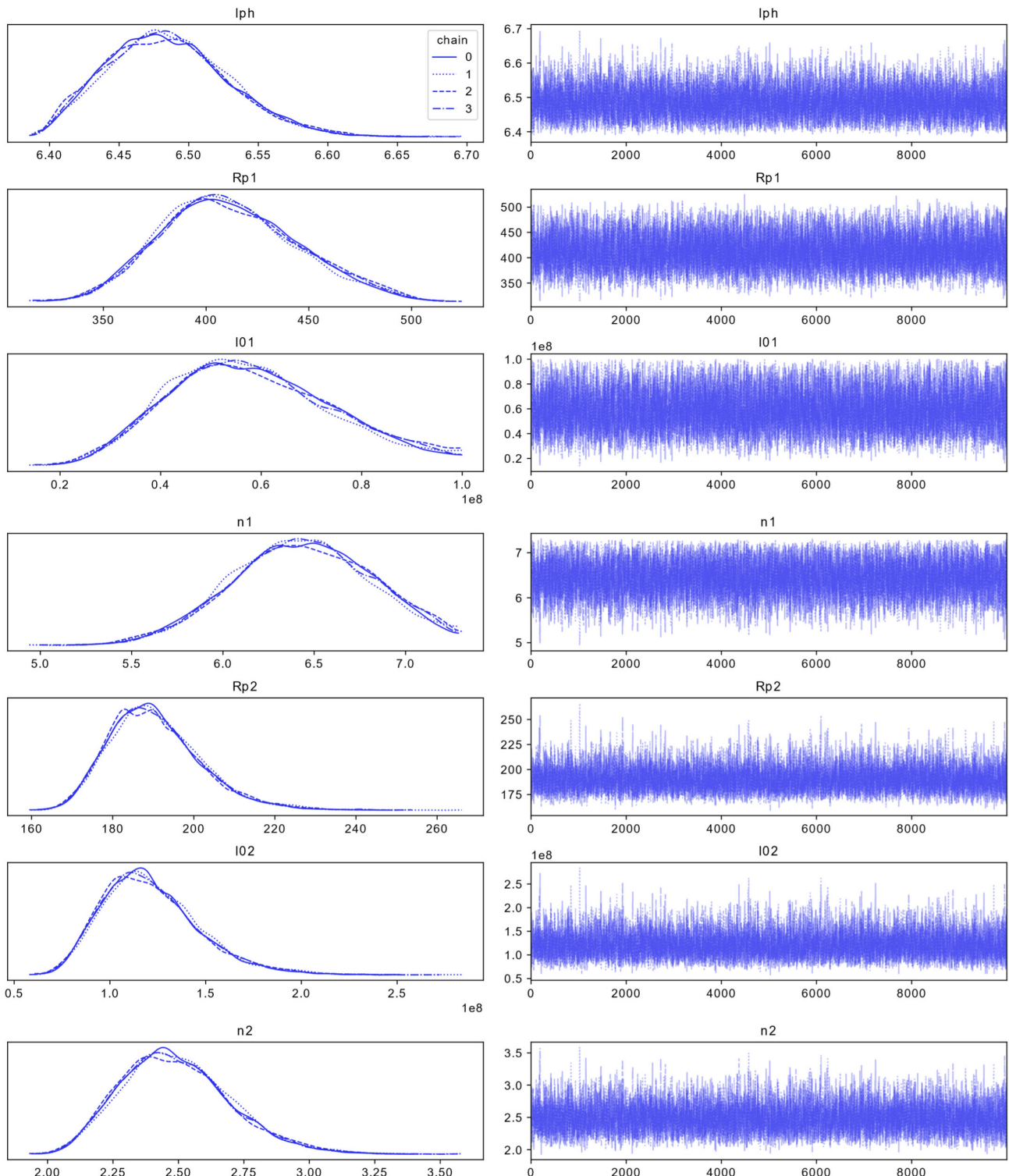


**Figure 5.** Kernel density estimates (left panels) and simulated traces (right panels) for each equivalent circuit parameter of the organic photovoltaic cell.<sup>[7]</sup>

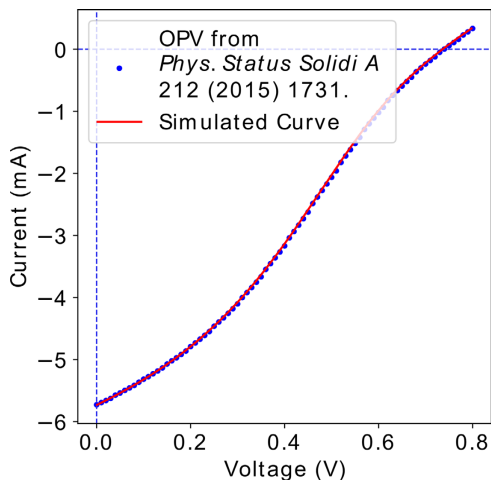


**Figure 6.** Experimental data (symbols) and simulated curve (line) for the organic photovoltaic cell from ref. [7]. The mean value of each parameter obtained by the Bayesian estimation was used to generate the simulated curve.

**Table 2.** Bayesian estimation of the equivalent circuit parameters of the organic photovoltaic cell from ref. [7].

	Mean value	Standard deviation	$\hat{R}$
$I_{ph}$ [mA]	6.49	0.04	1.0
$R_{p1}$ [ $\Omega$ ]	41.2	3.3	1.0
$I_01$ [pA]	$5.84 \times 10^7$	$1.63 \times 10^7$	1.0
$n_1$	6.44	0.38	1.0
$R_{p2}$ [ $\Omega$ ]	$1.91 \times 10^2$	$0.11 \times 10^2$	1.0
$I_02$ [pA]	$1.21 \times 10^8$	$0.26 \times 10^8$	1.0
$n_2$	2.49	0.21	1.0

meaning of this result is not clear at present and is a subject of future research.

## 4. Conclusion

In this article, we have shown the effectiveness of the Bayesian estimation in extracting the equivalent circuit parameters of the opposed two-diode model from the S-shaped current-voltage characteristics of a photovoltaic cell. Unlike the traditional non-linear least-squares method, the Bayesian estimation practically does not require any tuning of the initial values and gives the information on error of the estimates. Using this method, it has been demonstrated not only that it is possible to discriminate the difference between two theoretical curves that are almost identical in appearance but also that the ideality factors of the diodes can be determined from measured data.

## Acknowledgements

This work was partially supported by JSPS KAKENHI Grant Number JP18K04241.

## Conflict of Interest

The author declares no conflict of interest.

## Data Availability Statement

The data that support the findings of this study are available from the corresponding author upon reasonable request.

## Keywords

Bayesian estimation, equivalent circuit model, organic photovoltaic cell

Received: June 25, 2021

Revised: September 1, 2021

Published online: October 19, 2021

- [1] J. P. Charles, M. Abdelkrim, Y. H. Muoy, P. Mialhe, *Sol. Cells* **1981**, 4, 169.
- [2] M. Chegaar, Z. Ouennoughi, A. Hoffman, *Solid-State Electron.* **2001**, 45, 293.
- [3] A. Jain, A. Kapoor, *Sol. Energy Mater. Sol. Cells* **2004**, 81, 269.
- [4] D. Gupta, M. Bag, K. S. Narayan, *Appl. Phys. Lett.* **2008**, 92, 093301.
- [5] F. A. de Castro, J. Heier, F. Nüesch, R. Hany, *IEEE J. Sel. Top. Quantum Electron.* **2010**, 16, 1690.
- [6] G. del Pozo, B. Romero, B. Arredondo, *Sol. Ener. Mater. Sol. Cells* **2012**, 104, 81.
- [7] K. Tada, *Phys. Status Solidi A* **2015**, 212, 1731.
- [8] A. M. Humada, M. Hojabri, S. Mekhilef, H. M. Hamada, *Renew. Sustain. Energy Rev.* **2016**, 56, 494.
- [9] Y. Li, W. Huang, H. Huang, C. Hewitt, Y. Chen, G. Fang, D. L. Carroll, *Sol. Energy* **2013**, 90, 51.
- [10] K. Tada, *Phys. Status Solidi A* **2018**, 215, 1800448.
- [11] K. Nagata, S. Sugita, M. Okada, *Neural Netw.* **2012**, 28, 82.
- [12] R. E. Brandt, R. C. Kurchin, V. Steinmann, D. Kitchev, C. Roat, S. Levchenko, G. Ceder, T. Unold, T. Buonassisi, *Joule* **2017**, 1, 843.
- [13] I. Akai, K. Iwamitsu, M. Okada, *J. Phys.: Conf. Ser.* **2018**, 1036, 012022.
- [14] K. Tada, *Appl. Phys. Express* **2021**, 14, 046502.
- [15] M. D. Hoffman, A. Gelman, *J. Mach. Learn. Res.* **2014**, 15, 1593.
- [16] J. Salvatier, T. V. Wiecki, C. Fonnesbeck, *PeerJ Comput. Sci.* **2016**, 2, e55.
- [17] B. Romero, G. del Pozo, B. Arredondo, *Sol. Energy* **2012**, 86, 3026.
- [18] R. Corless, G. Gonnet, D. Hare, D. Jeffery, D. Knuth, *Adv. Comput. Math.* **1996**, 5, 329.
- [19] K. Roberts, (Preprint) arXiv:1504.01964v1 [math.NA], **2015**.
- [20] K. Roberts, (Preprint) arXiv:1601.02679v1 [Physics. Comp-Ph], **2015**.
- [21] T. Easwarakhanthan, J. Bottin, I. Bouhouc, C. Boutrit, *Int. J. Sol. Energy* **1986**, 4, 1.
- [22] K. Tada, *Org. Electron.* **2017**, 40, 8.